Polyurethane-Infiltrated Carbon Foams: A Coupling of Thermal and Mechanical Properties

Timothy J. Bunning,[1] Hong G. Jeon,[2]* Ajit K. Roy,[1] Kristen M. Kearns,[1] Barry L. Farmer,[1] Walter W. Adams[1]†

[1]*Air Force Research Laboratory, Materials and Manufacturing Directorate, Wright–Patterson Air Force Base, Ohio 45433*
[2]*Systran, Inc., Dayton, Ohio 45433*

Received 29 April 2002; accepted 11 July 2002

ABSTRACT: The thermal and mechanical properties of polyurethane-infiltrated carbon foam of various densities were investigated. By combining the high thermal conductivity of the carbon foam with the mechanical toughness of the pure polyurethane, a mechanically tough composite (relative to the unfilled foam) that could be used at higher temperatures than the polyurethane's degradation was formed. Both the tensile strength and the modulus increased by an order of magnitude for the composites compared to unfilled foam, while the compressive and shear strengths and moduli of the composites approached values exhibited by pure polyurethane. At both 300 and 400°C, the rectangular blocks of pure polyurethane lost their mechanical integrity due to decomposition in air. Thermogravimetric analysis confirms substantial initial weight loss above 290°C. Filled carbon foam blocks, however, maintain their mechanical integrity at both 300 and 400°C indefinitely, although the bulk of the rectangular block mass is polyurethane. Three different carbon foam densities are examined. As expected, the higher density foams show greater heat transfer. © 2003 Wiley Periodicals, Inc. J Appl Polym Sci 87: 2348–2355, 2003

INTRODUCTION

Carbon is pervasive in the natural surroundings, including the well-known extreme forms of graphite and diamond. In recent years, new forms of carbon, including C60 and carbon single- and multiwall nanotubes, are being examined extensively by many research groups. The use of carbon technology in structural applications is also well known; carbon fiber and carbon–carbon composites have been exploited in sporting goods and aircraft brakes due in large part to their low density. The high strength and/or stiffness of carbon-based materials arises from the graphitic structure of the individual carbon planes.[1]

One of the unique forms of carbon materials is microcellular (open-cell) bulk foam, originally developed by research scientists in Air Force Research Laboratory.[2] The microcellular foam exhibits isotropic material properties that are very important in a number of applications in which loading is nondirectional. These foams, available in a wide variety of densities, are lightweight, moisture-insensitive, and can be formed into complex structures by conventional machining techniques or by blowing into net shapes (www.poco.com; www.mercorp.com). In addition, low densities controlled by the porosity of the foam enable very large specific strength and modulus values.

These open-cell foams are blown from anisotropic pitch that aligns the graphitic planes within the interconnected struts.[3–13] Once blown, the foams are processed in a similar manner to pitch fibers. These foams are extremely tailorable, as a wide variety of thermal properties can be obtained, depending on the level of heat treatment and bulk density. Using a low-temperature (800°C) heat treatment, thermally insulating structures are formed, while using a high-temperature treatment (3,000°C) leads to highly conducting foams. In fact, bulk thermal conductivities on the order of several hundred W m^{-1}/K^{-1} have been obtained in the higher density foams (0.6 g/cm^3).

These attributes have led to a wide range of potential applications. High-conductivity foams are being examined as lightweight radiators and electronic thermal planes while low-conductivity structures are being investigated for thermal protection and insulating applications. Structural applications include mirrors, brakes, clutches, and a large number of sandwich structures in the automotive, marine, and aerospace industries. One drawback of these foams is their rela-

Correspondence to: T. J. Bunning (timothy.bunning@wpafb.af.mil).
**Present address:* Taylor Made-adidas Golf Co., Carlsbad, California 92008.
†*Present address:* Center for Nanoscale Science and Technology, Rice University, Houston, Texas 77005.

Journal of Applied Polymer Science, Vol. 87, 2348–2355 (2003)

tively low toughness compared to solid metal or polymeric materials. They are typically more brittle, and their toughness is several orders of magnitude smaller ($\sim 10^{-3}$ kJ/m^2) than a solid polymer or metal (10 kJ/m^2). Improving the mechanical properties of foams while maintaining a high thermal conductivity is thus the focus of several groups.[3–5,12,13] One approach to achieve better mechanical properties has been to infiltrate the open-cell foam with a wide variety of compounds, including polymers, metals, and ceramics.[14] Although shown to be feasible, little systematic study of the structure–property relationships has been reported for polymer-infiltrated foams. One such report includes a phase-change material in the pores of a blown carbon foam.[12]

In the work presented here, we infiltrate a polyurethane polymer into different density carbon foams in an attempt to increase the mechanical properties of the foam while allowing the use of the polymer at or above its decomposition temperature for a limited amount of time in conjunction with a heat sink. The premise was that the foam's high bulk thermal conductivity would allow for heat dissipation (to a heat sink) while concurrently increasing the strength of the composite. We report on several sets of thermal experiments that clearly indicate the composite can be operated above the degradation temperature of the infiltrated polyurethane. We also report on the shear, compression, and tensile mechanical properties of the pure polyurethane, unfilled carbon foams, and polyurethane-reinforced carbon foams.

EXPERIMENTAL

Three different density carbon foams were purchased from MER (Tucson, AZ). The apparent bulk and specific densities of as-received foam materials were measured from dry and water-infiltrated foams, respectively. The measured bulk densities of the three foams were 0.14, 0.25, and 0.34 g/cm^3; for the remainder of the article, these foams will be referred to as A, B, and C, respectively. The apparent specific gravities of A, B, and C, obtained using Archimedes displacement method (ASTM C 373-72), are 1.6, 1.8, and 1.9, respectively. All three foams in this study show nearly the same specific gravity as carbonized foam (1.85), but lower than graphitized foam (2.0). The calculated open porosity of A, B, and C were 92%, 86%, and 82%, respectively. The castable polyurethane (PU) employed was a two-component mixture (Royalcast 3101) supplied by Uniroyal. The foam was filled with the mixture using vacuum infiltration under a mild vacuum ($\sim$100 kPa for 6 min), then annealed at 100°C for 16 h to complete the curing. The foam samples before and after PU infiltration were examined using conventional optical and scanning electron microscopy. Thermal degradation of PU and PU-filled foams was characterized using a TA Instrument TGA at a heating rate of 10°C/min in air. The isothermal weight loss was measured for PU and PU-filled foam samples with dimensions of 32 $\times$ 7 $\times$ mm. For the kinetic experiments, one end was placed on a hot plate at the temperature of interest while the other end was placed in contact with a heat sink consisting of a copper block circulating ice water. The weight of sample was measured as a function of time, and the temperature at various locations along the specimen was measured

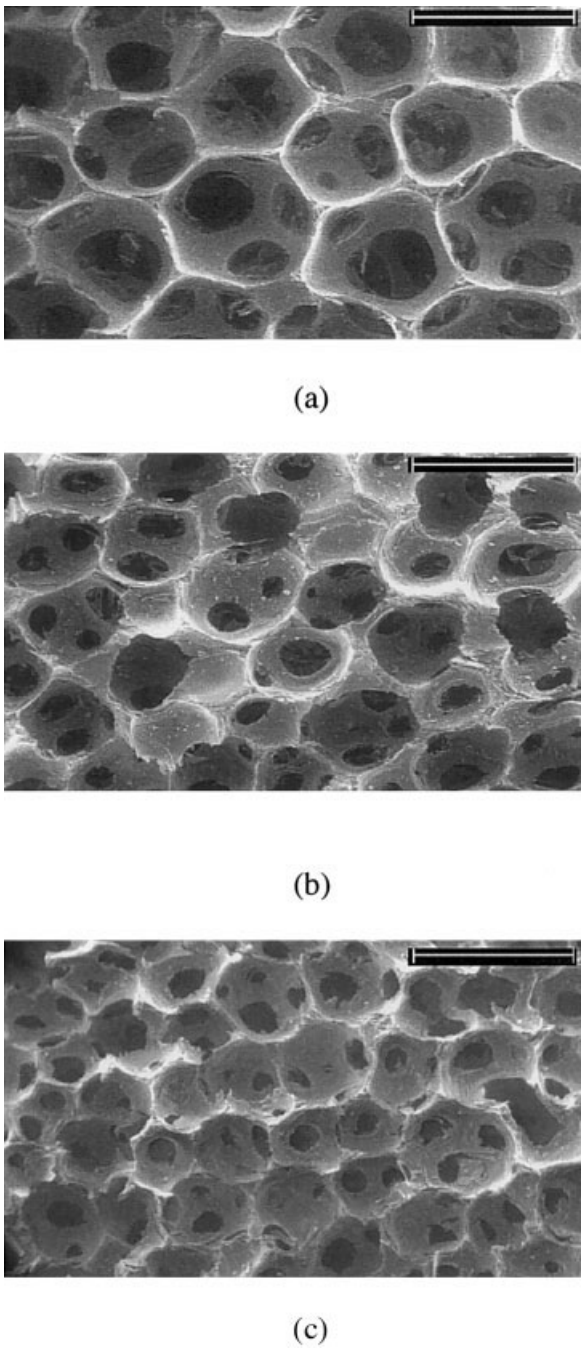

Figure 1 Scanning electron micrographs (15 kV) of fracture surfaces from unfilled purchased foams (a) A, (b) B, and (c) C. Scale bar corresponds to 1 mm.

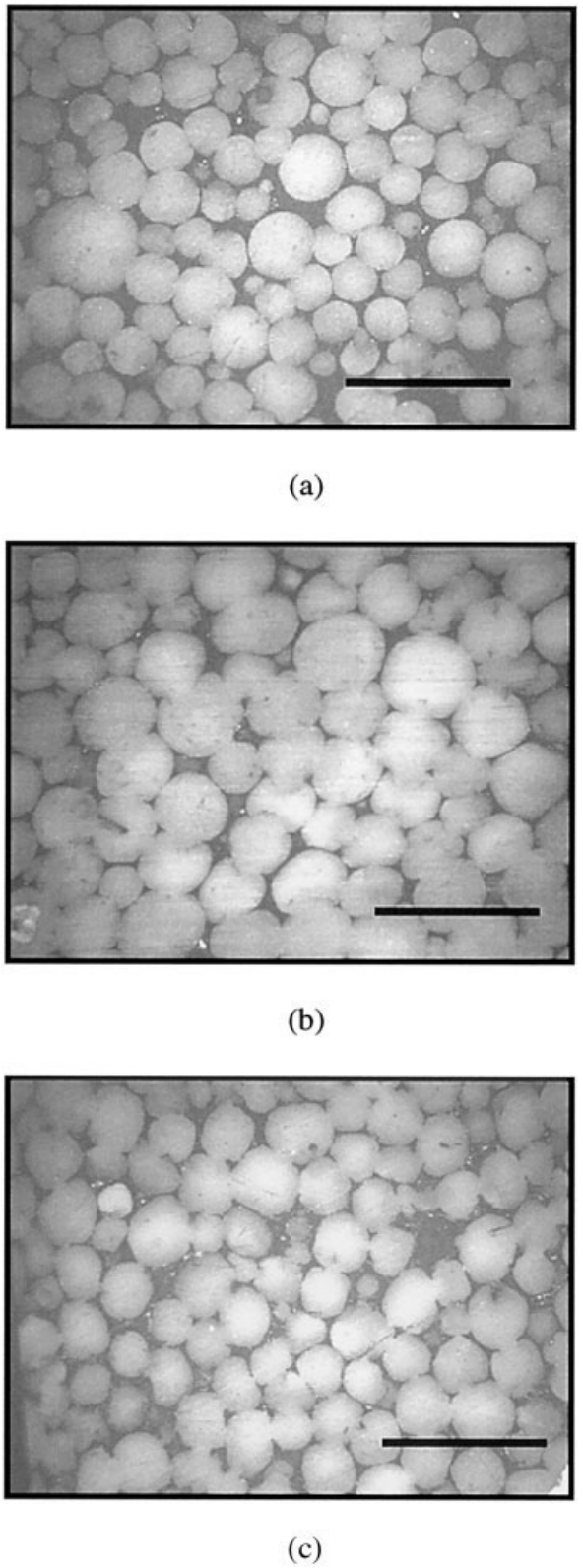

Figure 2 Optical micrographs of polished foam surfaces (a) A_f, (b) B_f, and (c) C_f after filling with polyurethane. Scale bar corresponds to (a) 2, (b) 1, and (c) 1 mm.

using a noncontact infrared thermometer (Mikron), which has a spot size diameter of ~2 mm.

Because of the expected bulk (or macroscopic) isotropic properties of neat foam as well as the foam filled with PU, only two of the three material properties (Young's modulus, shear modulus, and Poisson's ratio) define the structural behavior of the material. The tensile (or compression) and shear properties (stiffness and strength) are the two properties measured using the test configurations developed by Roy et al.[15–17] Poisson's ratio of the material can be determined from the measured values of the tensile and shear moduli using the isotropic assumption. Due to the high porosity of the material, the tensile coupons prepared from the material could not be directly gripped in the testing frame using hydrostatic end grips. In order to apply a uniform displacement on the foam sample subjected to a tensile load, tab materials were bonded to the two ends of the foam sample. The specimens were pin-loaded through the tab materials to eliminate any bending of the specimen during loading. Due to the high porosity of the material, standard strain measuring devices such as clip extensometers and strain gages could not be used to measure strain. Thus, the strain applied to the specimen was calculated from the machine head displacement, assuming the amount of strain in the bond between the tab and the foam is negligible compared to that of the material in the gage section. To measure the compressive modulus and strength, ASTM standard C 365 was used to measure compressive modulus and strength. In this test, a specimen in the configuration of a cube is loaded in compression between two platens of a load frame, and the strain is measured using the machine head displacement.

None of the standard test configurations [single rail, double rail (ASTM D 4255)], or Iosipescu (ASTM D

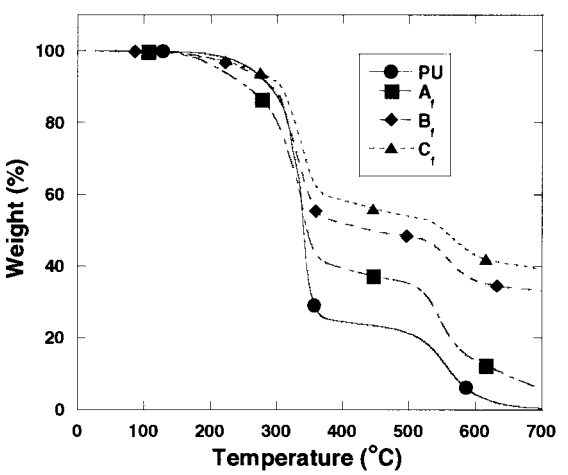

Figure 3 Thermogravimetric analysis (in air) of the pure bulk polyurethane material and the three filled foam samples. The first large-scale decomposition of the polyurethane material occurs near 300°C.

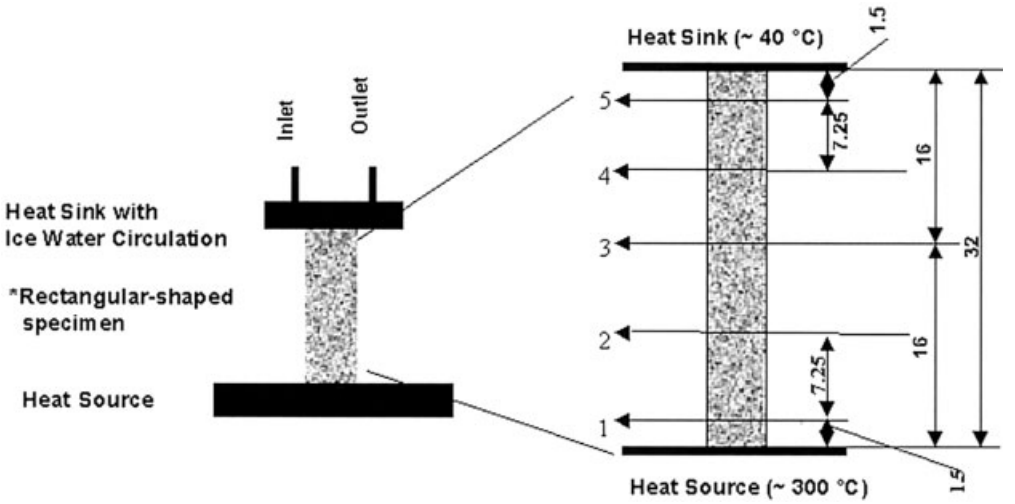

Figure 4 Schematic of the heating sink geometry and the polyurethane-filled foam samples used in the heat sink experiments. Positions 1–5 correspond to the locations the sample was probed using a noncontact infrared thermometer.

5379)] are applicable to measuring shear stiffness and strength of these carbon foams due to their brittleness. The shear properties (modulus and strength) of the material were measured with a shear-testing fixture specially designed to measure shear properties of porous material.[17] In order to eliminate excessive stress concentration in the foam ligaments in the vicinity of the loading locations, the test fixture uses cylindrical specimens of circular cross section. The shear strain was imposed by applying torque through the specimen's two ends. Since strain gages could not be installed on the specimen surface, shear strain was determined from the specimen end rotation with a special device to obtain an angular rotational resolution of 0.005°. Further, to relieve the axial constraint while twisting the specimen (applying torque), the specimen-gripping end attached to the load cell is mounted on a linear roller.

RESULTS AND DISCUSSION

Figure 1 shows the SEM pictures taken from fractured samples of unfilled foams, showing relatively uniform pore sizes and substantial interconnectivity. The average diameters of A, B, and C based on SEM pictures are 900, 650, and 550 μm, respectively. As expected, the average diameter of open pores decreases with increasing bulk density. Upon PU filling, the bulk densities of the A, B, and C foams increase substantially from 0.14 to 1.14, 0.25 to 1.18, and 0.34 to 1.21 g/cm^3, respectively (labeled A_f, B_f, and C_f for the remainder of the article). Based on the bulk density of pure polyurethane of 1.1 g/cm^3, the calculated percentages of open pores filled with PU are 98%, 96%, and 96% for A_f, B_f, and C_f, respectively. Figure 2 presents optical micrographs of the polished surface

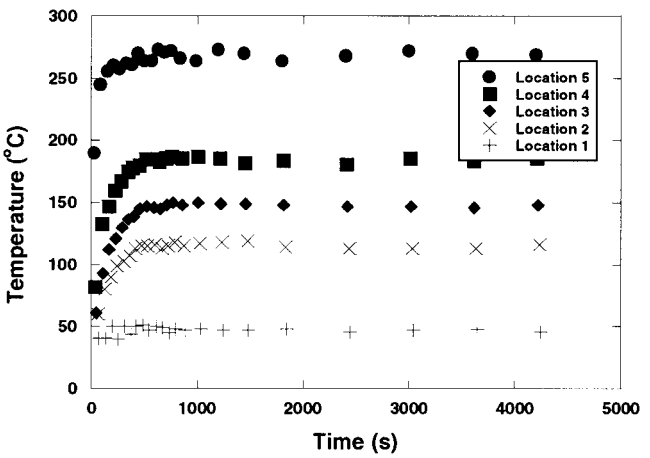

(a)

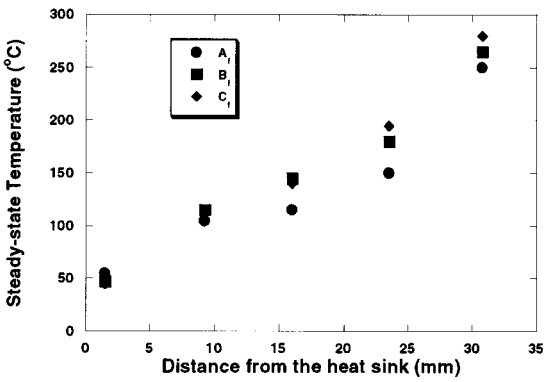

(b)

Figure 5 The temperature evolution as a function of time for each location as defined in Figure 4 for sample B_f (a) and the final steady-state temperature of the three filled foam samples as a function of location on the rectangular samples (b).

TABLE I
Initial Heating Rates (°C/min) Taken as a Function of Position along Composites of PU-Filled Carbon Foams

Position	A_f	B_f	C_f
1	4.4	5.9	6.4
2	1.1	1.1	1.4
3	0.8	0.6	0.7
4	0.7	0.4	0.4
5	0.3	0.1	0.0

of A_f, B_f, and C_f. As can be seen, all three foam samples are nearly completely filled with PU.

The thermal decomposition behavior of the polyurethane and the PU-filled foams is shown in Figure 3. The decomposition process is a two-step process with a large initial weight loss occurring between 290 and 350°C, corresponding to decomposition of PU. A second, smaller weight loss occurring above 500°C corresponds to carbon oxidation. The filled-foam decomposition curve exhibits the same shape, but is shifted with respect to the fractional weight loss. Based on the weight loss at 425°C, the weight percentages of PU were calculated for A_f, B_f, and C_f as ~88, ~73, and ~67%, respectively. These are consistent with the measured values of 86%, 77%, and 71% for A_f, B_f, and C_f, respectively, obtained from the porosity and bulk density of unfilled foams and PU.

In order to examine the heat dissipation from PU by a large thermal conductivity foam, a set of experiments was conducted in the presence of a heat source and a heat sink. Shown schematically in Figure 4, a block of filled foam with dimensions of $32 \times 7 \times 7$ mm was placed between the surface of a hot plate at 300°C and a continuously cooled copper block. Note that the temperature of the heat source is above the decomposition temperature of PU. Both the temperature as a

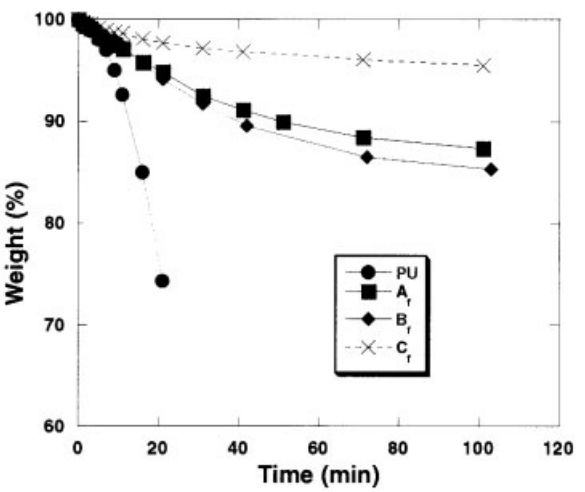

(a)

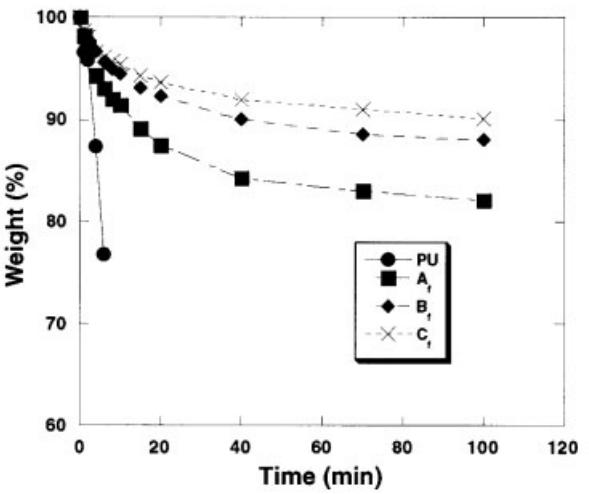

(b)

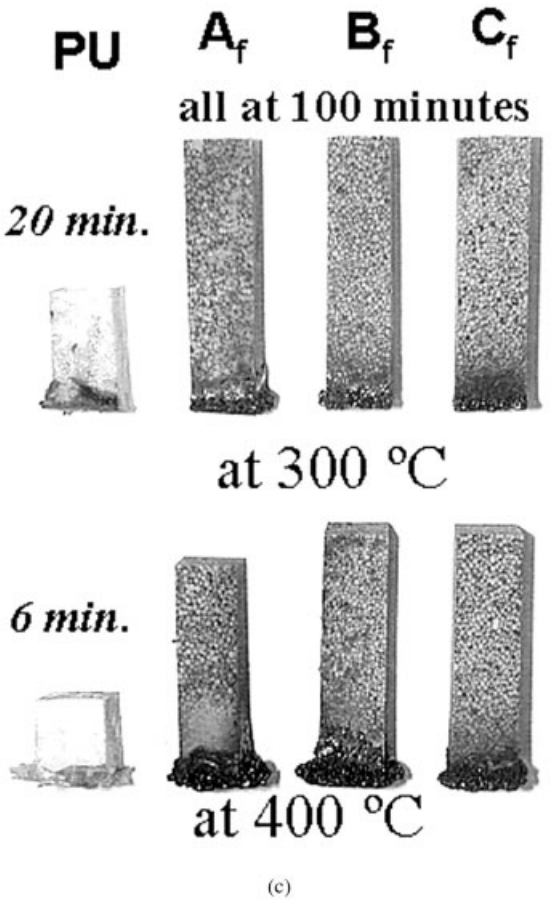

(c)

Figure 6 Weight loss as a function of time for the pure bulk polyurethane and filled foam rectangular samples at both 300 (a) and 400°C (b). Image (c) of the rectangular samples tested in (a) and (b).

TABLE II
Mechanical Properties of Polyurethane and Filled and Unfilled Carbon Foams

Sample	Tensile strength (MPa)	Tensile modulus (MPa)	Compressive strength (MPa)	Compressive modulus (MPa)	Shear strength (MPa)	Shear modulus (MPa)
PU	35	1,700	40	750	10-50[a]	570[b]
A	Not measurable	Not measurable	0.3	50	0.25	52
B	0.5	950	1.9	53		
C	0.7	1,100	2.3	68		
A_f	9.5	1,550	39	820	9.4	460
B_f	10.5	4,400				
C_f	9.5	4,000	41	810		

[a] Typical polymer value (not measured).
[b] Calculated from the measured tensile values.

function of position and the weight of the sample as a function of time were measured. Figure 4 shows the positions along the length of the block where the temperature was measured.

An example of the spatial–temperature variation is shown in Figure 5(a) for the B_f sample. The temperature rises quickly at all positions, with the magnitude of the change largest for the locations closest to the heat source. A steady-state temperature is reached earliest at regions closest to the heat sink and progressively requires longer times with increased distance from the heat sink. The initial slopes for each position (shown in Fig. 4) were measured from the early time data and are shown in Table I. As expected, the higher density foam exhibits a higher initial rate due to more surface area in which heat could be conducted. The difference between these initial rates with density diminishes at position 5 due to the effects of the heat sink. Figure 5(b) shows the steady-state temperature obtained at each spot for the three different foams. Steady-state one-dimensional heat transport theory would predict a linear relationship. Although a slight dip occurs, particularly for the lowest density foam (A_f), the shape of curves is approximately linear as expected. Again, at the locations closest to the heat source, the highest density foam (C_f) with the highest apparent thermal conductivity exhibits a slightly larger steady-state temperature.

Even more telling is the weight loss curves as a function of time at 300°C and at a substantially higher temperature, 400°C, as shown in Figure 6(a) and (b), respectively. At both temperatures, the polyurethane block exhibits substantial weight loss and essentially burns away. The images of samples exposed at both temperatures are shown in Figure 6(c). As can be seen, the PU samples collapse at both temperatures, which is expected because both temperatures are above the degradation temperature of polyurethane. Interestingly, the PU-filled foams retain most of its mass, although the majority is composed of PU. Thus, these results suggest that the PU is not decomposing. The curves presented in Figure 6(a,b) indicate that after an initial small weight loss, the samples do not show any significant weight loss. Figure 6(c) indicates that a stable char is formed at the surface in contact with the heat source. In contrast to PU-filled foam, pure PU does not show stable char formation. These results suggest that polymer-filled foams can be utilized at substantially higher temperatures than the degradation temperature of the neat polymer. This is due to the large effective thermal conductivity of the filled samples. Efforts to date to measure the inherent bulk thermal conductivity of either the unfilled or the filled foams have been unsuccessful, primarily because of the heterogeneous nature of the surfaces of the specimens.

TABLE III
Comparison of Predicted Tensile Modulus of Filled Foam with the Measured Values

Sample	Foam Open Porosity $P = 100 \times (1 - V_{fm})$ (%)	Tensile modulus, E (MPa)	Effective foam ligament modulus, $E_{fm} = E/V_{fm}$ (MPa)	Predicted filled foam tensile modulus (MPa) Series Model $\frac{1}{E_f} = \frac{V_{fm}}{E_{fm}} + \frac{V_{pu}}{E_{pu}}$	Predicted filled foam tensile modulus (MPa) Parallel Model $E_f = V_{fm}E_{fm} + V_{pu}E_{pu}$
PU		1,700			
B	86	950	6,790		
C	82	1,100	6,100		
B_f		4,400		1,900	2,400
C_f		4,000		1,950	2,500

The utilization of a polymer-filled foam above the polymer degradation temperature is only of benefit if the polymer imparts some useful property to the composite. Knowing that the mechanical strength of the unfilled foams is poor, a systematic investigation of mechanical properties was investigated. Table II shows the summary of mechanical properties of PU, unfilled foams, and PU-filled foams. The tensile strength and modulus of the pure PU were measured to be 35 and 1,700 MPa, respectively. The tensile properties of samples B and C were barely measurable, while sample A (the least dense) was not. Upon filling, a substantial increase in both strength and modulus over that of unfilled foam is observed. PU-filled foams (B_f and C_f) exhibit tensile moduli larger than the pure PU. To develop an understanding of the mechanism for the substantial increase in modulus of filled foam B_f and C_f, the contribution of infiltrated PU in foam was analyzed by means of one-dimensional series and parallel models. The predicted values of the tensile modulus of the filled foam B_f and C_f are shown in Table III. E_{fs} and E_{fp} denote the filled foam tensile modulus predicted by using series and parallel model, respectively. In the expressions for the series and parallel model, E_{fm} denotes the effective foam ligament tensile modulus, E_{pu} is that for PU, and V_{fm} and V_{pu} are the volume fraction of foam and PU in filled foam, respectively. It can be seen from Table III that both the series and parallel models grossly underpredict the measured tensile modulus of the filled foam. This implies that the constraining mechanism imposed by the foam ligament on PU is not one-dimensional; hence, one-dimensional models are not applicable to analyzing the behavior of filled foam. Actually, due to the three-dimensional network of foam ligaments, the deformational constraint imposed by the foam ligaments on PU is truly three-dimensional. Thus, to analyze the filled foam behavior, a three-dimensional deformation of a unit cell of foam ligaments with PU filling the open space of the foam unit cell needs to be analyzed.

The relatively small modulus of A_f is hypothesized to be due to poor adhesion between PU and cell walls of foam. Figure 7 presents the SEM micrographs of fracture surface of all three PU-filled foams, showing relatively better adhesion for B_f and C_f. Relatively smooth fracture surfaces were observed for A_f, while substantial roughness was observed for B_f and C_f. One possible explanation would be that compared to B_f and C_f, there was more PU shrinkage in A_f during the curing process due to the larger pore size, leading to more delamination between polymer and cell walls. Although not explored in any detail in this work, these results indicate that the wetting and interfacial bonding properties are important factors dictating the success of mechanical reinforcement.

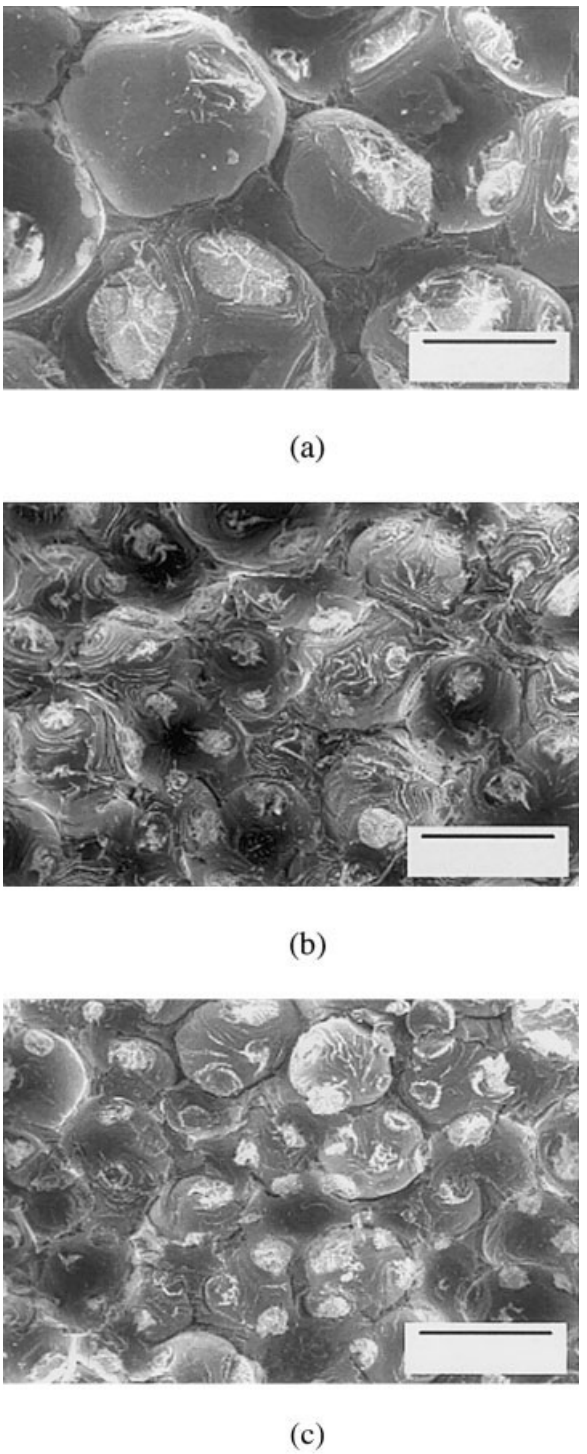

Figure 7 Optical micrographs of the fracture surface of the three filled foam samples (a) A_f, (b) B_f, and (c) C_f. Scale bar corresponds to 500 μm.

Compressive and shear strength and moduli are also shown in Table II. For both cases, pure PU has substantially higher values than any of the unfilled foams. In fact, the unfilled foams are very weak, making measurements difficult to perform. Upon filling, values commensurate with the pure PU are obtained.

Thus, filling the foams with the polyurethane substantially improves the mechanical properties relative to the unfilled foams.

CONCLUSIONS

A composite consisting of a high thermal conductivity carbon foam and a polyurethane incorporates the utility of both materials. As a result of PU infiltration, the mechanical properties of filled carbon foam were substantially improved. The tensile strength and moduli were increased an order of magnitude while the compressive and shear properties of the filled systems essentially mimic that of the pure polyurethane. The high thermal conductivity of the carbon foam allows for heat to be dissipated from the polymer easily when in the presence of a heat sink. This helps minimize the PU degradation at temperatures substantially higher than the pure PU decomposition temperature. This allows for utilization of these composites at temperatures higher than the maximum use temperature of the neat polymer.

References

1. Edie, D. D. In Carbon Fibers, Filaments, and Composites; Figueredo, J. L., Ed.; Kluwer Academic Publishers: New York, 1990; p. 43.
2. Hall, R. B.; Hager, J. W. In 21st Biennial Conference on Carbon Extended Abstracts; American Carbon Society; Elsevier Science: Tarrytown, NY, 1993; p. 100.
3. Klett, J. Proc Sampe 1998, 43, 745.
4. Klett, J.; Conway, B. Proc Sampe 2000, 45, 1933.
5. Klett, J.; Hardy, R.; Romine, E.; Walls, C.; Burchell, T. Carbon 2000, 38, 953.
6. Hager, J. W.; Lake, M. L. MRS Proc 1992, 270, 29.
7. Hager, J. W.; Anderson, D. P. In Proceedings of the 21st Biennial Conference on Carbon; American Carbon Society; Elsevier Science: Tarrytown, NY, 1993; p. 102.
8. Mukhoppadhyay, S. M.; Mahadev, N.; Joshi, P.; Roy, A. K.; Kearns, K. M.; Anderson, D. P. J Appl Phys 2002, 91, 3415.
9. Kearns, K. M.; Anderson, D. P. In Proceedings of the 11th International Conference on Composite Materials; Scott, M. L.; Woodhead Publishing Ltd.: Cambridge, UK, 1997; p. 825.
10. Kearns, K. M. U.S. Pat. 5, 868, 974 (1999).
11. Kearns, K. M. U.S. Pat. 5, 961, 814 (1999).
12. Klett, J. W.; Burchell, T. D. U.S. Pat. 6,037,032 (2000).
13. Klett, J. W. U.S. Pat. 6,344,159 (2002).
14. Klett, J.; Klett, L.; Strizak, J.; Williams, M.; McMillian, A.; Valencia, J.; Creeden, T. Presented at the 24th Annual Conference on Ceramic, Metal and Carbon Composites, Materials, and Structures, Cocoa Beach, FL, January 24–28, 2000.
15. Roy, A. K.; Pullman, D.; Kearns, K. M. Proc Sampe 1998, 43, 774.
16. Sihn, S.; Roy, A. K. Presented at the Second Annual Carbon Foam Workshop, Wright-Patterson AFB, OH, November 2–3, 2000.
17. Roy, A. K.; Camping, J. D. Exp Mech, 42, 4, 1, 2002.